

# LOSS MODELLING AND EXPERIMENTAL VERIFICATION OF A 98.8% EFFICIENCY BIDIRECTIONAL ISOLATED DC-DC CONVERTER

Rakesh Ramachandran, Morten Nymand

University of Southern Denmark, Odense, Denmark, Email:rar@mmmi.sdu.dk

## ABSTRACT

High efficiency in power converters means less power wasted, which implies reduction in heat sink requirement, thereby small in size and less in weight. This power loss reductions in space application leads to smaller solar panels and less fuel on-board, hence reduces the spacecraft size, weight and launch cost. One of the major challenges for power converters in space application is to boost their efficiency, to reduce thermal dissipation problems.

In this paper, design and implementation of an ultra-high efficiency isolated bi-directional dc-dc converter utilizing GaN devices is presented. Loss modelling of the GaN converter is also included in this paper. The converter has achieved a maximum measured efficiency of 98.8% in both directions of power flow, using the same power components. Hardware prototype of the converter along with the measured efficiency curve is also presented in this paper.

## 1. INTRODUCTION

Solar energy is a major source of energy for the satellite in orbit. A bidirectional dc-dc converter is highly desirable to charge the battery with solar energy and in eclipse period to power the satellite equipment.

Some of the mandatory requirement for a converter used in satellite includes high conversion efficiency to reduce thermal dissipation problems, electrical isolation between input and output stages and low mass [1], [2]. Since, the size, reliability and efficiency of the overall system mainly depend on the power losses of the converter; efficiency is a key parameter in designing such a dc-dc converter.

GaN FETs have lower switching loss and conduction loss compared to Si MOSFET. Hence the efficiency of the whole converter can be increased to reduce the thermal dissipation and size, thereby making it more compact [3], [4].

Various bidirectional converters to achieve high efficiency have been discussed in the literature [5]-[7]. In [5], a 2 kW, 20 kHz with current doubler topology is presented. The maximum efficiency achieved is 96% at 600W in boost mode and 96% at 1200W in buck mode. A 1 kW resonant bidirectional converter is presented in

[6] with an efficiency of 97.5% in forward and 97% in backward direction.

This paper presents an ultra-high efficiency isolated dc-dc converter. GaN devices are used as the switching device to realize the hardware prototype of the converter. This paper also discusses the design of high efficiency magnetics along with design considerations of using GaN FETs as the switching device. The loss modelling of the GaN converter is also presented in the paper.

The proposed converter is a bidirectional converter which allows the power flow in both directions using the same power components. The hardware prototype of a 1.7 kW GaN converter is presented in this paper. The measured maximum efficiency of the converter is 98.8% in both the directions of power flow. The converter has also achieved an efficiency of above 98.5% over a wide range of output power.

## 2. ISOLATED BI-DIRECTIONAL DC-DC CONVERTER

The circuit diagram of an isolated full bridge bidirectional dc-dc converter is shown in Figure 1.

The converter works as an isolated buck converter in forward direction and isolated boost converter in backward direction. Figure 2 show the operational waveforms of the bidirectional converter in both directions of power flow.

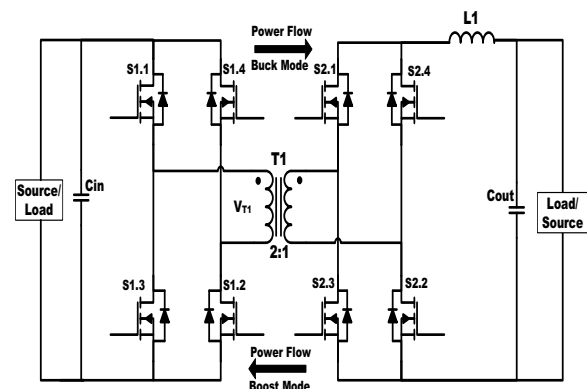


Figure 1. Isolated full-bridge bidirectional dc-dc converter

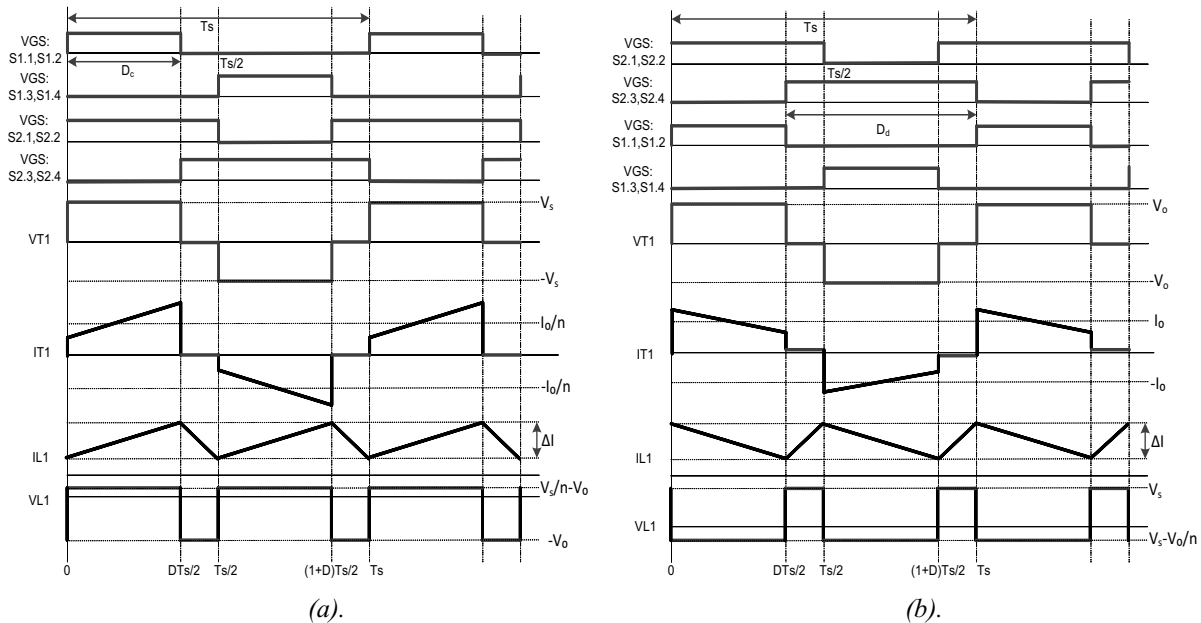


Figure 2. Operational waveforms of an isolated bidirectional dc-dc converter, (a) buck mode and (b) boost mode

The operation principle of the converter in buck mode and boost mode are explained in [8] and [9], respectively.

### 3. CONVERTER DESIGN

In buck mode of operation, the designed isolated dc-dc converter has an input voltage of 130V and output voltage of 52V. The 130V side is referred as the high voltage side and corresponding secondary is referred as the low voltage side. The design specifications of the converter are shown in Table.1.

Output Power	1.7 kW
High Voltage Side	130 V
Low Voltage Side	52 V
Switching Frequency	50 kHz
Transformer Core	Ferroxcube EE55/28
Inductor Core	Kool M $\mu$ E40
HV side GaN FETs	EPC2010C
LV side GaN FETs	EPC2001C

Table 1. Bidirectional converter design considerations

#### 3.1. Transformer

High frequency transformer galvanic-ally isolates the source and the load. In order to have high efficiency in transformer, both core loss and copper loss has to be reduced. Ferrites E-core has been selected as the core material to have lower core loss. The major challenge to achieve high efficiency in power transformer is to have very low ac-resistance. Extensive interleaving of primary and secondary reduces the proximity effect and hence dramatically reduces the ac-resistance of the transformer

[7]. Extensive interleaving with fewer turns also reduces the leakage inductance of the transformer. Hence, low ac-resistance and low leakage inductance increases the efficiency of the transformer even at higher power levels.

#### 3.2. Inductor

In an isolated dc-dc converter, storage inductor is designed to operate with a dc bias current with a small ac ripple current. Core materials with high saturation flux will help in minimizing the inductor size and increasing the efficiency. Thus, Magnetics Kool M $\mu$  is selected for the inductor core. For high dc bias current application, copper cross section has to be higher; hence copper foils are used for the winding. In order to reduce the ac-winding loss, two winding technique, is used for inductor design, explained in [11]. A thin ac winding is used to reduce the ac resistance and a thick dc winding to reduce the dc resistance. Thereby reducing the losses and hence high efficiency in inductor can be realized.

#### 3.3. GaN FETs

GaN FETs are used as the switching devices. 200V and 100V FETs are used at the high voltage and low voltage sides of the transformer respectively. In order to reduce the conduction losses, four devices are used in parallel.

One of the main reasons for selecting GaN device is that they have zero reverse recovery losses compared to Si MOSFET. This is highly advantageous in low voltage high current synchronous rectification applications. Synchronous rectification helps in improving the efficiency of the overall converter.

The major challenges in using GaN FETs in high power

converters are the optimum PCB layout design and the design of gate drive circuit. They have a very small threshold voltage and low gate-source voltage rating. A small noise injected into the gate of these devices, due to any parasitic inductance, can cause the device to turn-on or turn-off inadvertently and can cause damage to the whole converter.

LM5114 from Texas Instruments is chosen as the driver for the GaN devices. These drivers are capable of driving multiple GaN FETs due to their large sink current capability. Each driver drives four parallel devices. They also have a split gate output, which provides flexibility to adjust the turn-on and turn-off independently. The driver is compactable with TTL/CMOS signals and can withstand voltages up to 14V. This allows the driver to provide input directly from any PWM controller. LM5114 has a fast switching speed and minimized propagation delay of 12nS. An LCR tank circuit is usually formed with the parasitic source impedance, gate capacitance and the drive pull down path. This LCR tank circuit causes ringing in the gate of the GaN devices, an optimized resistor is used to damp this ringing [10].

#### 3.4. Filter capacitors

Ceramic capacitors are used as the filter capacitors at both high voltage and low voltage sides of the converter. Compared to electrolytic capacitors, ceramic capacitors occupies very small volume. This helps in improving the power density of the converter. Even though the capacitance value in ceramic capacitor reduces with the dc-bias voltage, twice the number of capacitors has been used, which provides enough capacitance at both high voltage and low voltage side of the converter. These capacitors also have a very low ESR value, hence contribute to very low losses.

## 4. ANALYTICAL LOSS MODELLING

Loss modelling of individual power components is performed to predict the performance characteristics of the converter. The losses in the converter are dependent on many functions, mainly on switching frequency, input voltage and load current. The major source of power losses in an isolated converter are distributed among magnetics and the power semiconductor devices.

The power loss in individual components, transformer, inductor and semiconductor devices, can be expressed by a second order quadratic equation as a function of output current,  $I_o$ .

$$P_{loss} = k_o + k_2 I_o^2 \quad (1)$$

where,  $k_o$  is the idle losses and  $k_2$  is the loss factor associated with the resistive losses in the respective power component.

The loss modelling of the individual power components are discussed below.

### 4.1. Transformer

The idle loss in the transformer is mainly the core loss. The core loss can be calculated using the Steinmetz formula [12],

$$P_v = k f^\alpha B^\beta \quad (2)$$

where,  $P_v$  is the power loss per unit volume,  $B$  is the flux density,  $f$  is the frequency, and  $k$ ,  $\alpha$ ,  $\beta$  are the material parameters.

The ac-resistance of the transformer can be expressed by the equation [9]

$$R_{ac} = R_{dc} \varphi \frac{\sinh 2\varphi + \sin 2\varphi}{\cosh 2\varphi - \cos 2\varphi} + \frac{2(m^2 - 1)}{3} \varphi \frac{\sinh \varphi - \sin \varphi}{\cosh \varphi + \cos \varphi} \quad (3)$$

where,  $\varphi = h/\delta$ ,  $h$  is the height of the conductor,  $\delta$  is the penetration depth,  $R_{ac}$  is the ac resistance of the winding,  $R_{dc}$  is the winding dc resistance and  $m$  is the number of layers in the winding.

The rms current through the primary winding can be written as

$$I_{RMS,tfr} = \frac{I_o}{n} \sqrt{D_c} \quad (4)$$

where,  $n$  is the turns ratio and  $D_c$  is the duty cycle.

The resistive losses in the transformer can be calculated from the ac-resistance and the RMS current through the winding.

The transformer power loss equation can be expressed as a function of output current,  $I_o$  as

$$P_{tfr} = 2.18 + 0.00262 I_o^2 \quad (5)$$

### 4.2. Inductor

Similar to transformer, inductor losses also includes both core loss and winding loss. Core loss can be estimated from the Steinmetz equation as given in (2).

Since the inductor is designed using a two-winding technique, the winding losses includes both ac and dc-winding losses. The losses are calculated assuming  $\frac{2}{3}$  of the ac ripple current flows through the ac winding and the remaining  $\frac{1}{3}$  flows through the dc-winding [11].

The power loss equation for the inductor is given as

$$P_{I_{dr}} = 0.83 + 0.001175I_o^2 \quad (6)$$

### 4.3. GaN FETs

The losses in GaN FETs include both switching loss and resistive loss.

Gate drive losses and output capacitive losses are included in the switching losses and can be estimated from the equation given below.

Gate drive loss is given by,

$$P_{drive} = V_d Q_G f \quad (7)$$

where,  $V_d$  is the drive voltage and  $Q_G$  is the total gate charge and  $f$  is the switching frequency.

The analysis of capacitive switching loss in an isolated dc-dc converter is explained in [13]. From [13], the capacitive switching loss in the GaN FETs can be written as,

$$P_{cap(loss)} = \{2Q_{oss,p(V_{in})} - [\frac{5}{8}Q_{oss,p(\frac{3V_{in}}{8})} + \frac{3}{8}Q_{oss,p(\frac{5V_{in}}{8})}]\} + \frac{2}{n}Q_{oss,s(\frac{V_{in}}{n})} \} V_{in} f \quad (8)$$

where,  $Q_{oss,p(V_{in})}$  is the output charge of four parallel primary switches at  $V_{in}$ ,  $Q_{oss,p(\frac{5V_{in}}{8})}$  is the output charge of four parallel primary switches at  $\frac{5V_{in}}{8}$ ,  $Q_{oss,p(\frac{3V_{in}}{8})}$  is the output charge of four parallel primary switches at  $\frac{3V_{in}}{8}$ ,  $Q_{oss,s(\frac{V_{in}}{n})}$  is the output charge at  $\frac{V_{in}}{n}$  of four parallel secondary switches.

Resistive losses in GaN FETs can be estimated from the on-resistance of the respective FETs and the RMS current through them.

Losses in the high voltage FET can be calculated by,

$$P_{HLOSS} = R_{DS(ON)H} \frac{P_o \sqrt{D} C}{n_c V_o} \quad (9)$$

where,  $R_{DS(ON)H}$  is the on-resistance of high voltage FETs,  $P_o$  is the output power, and  $V_o$  is the output voltage in buck mode of operation.

Similarly, the conduction losses in low voltage FET can be expressed as,

$$P_{LLOSS} = R_{DS(ON)L} \frac{P_o}{V_o} \quad (10)$$

where,  $R_{DS(ON)L}$  is the on-resistance of low voltage FETs.

The power loss equation for the GaN FETs can be written as

$$P_{GaN} = 3.79 + 0.00652I_o^2 \quad (11)$$

The dielectric loss in the filter capacitors can be calculated by,

$$P_{di\_cap} = 2\pi f C V^2 \tan \delta \quad (12)$$

where,  $C$  is the filter capacitance value,  $V$  is the voltage across the capacitor and  $\tan \delta$  is the loss tangent or dissipation factor.

So the total loss in the converter can be expressed as a second order quadratic equation as

$$P_{tot} = 6.8 + 0.0117I_o^2 \quad (13)$$

From the above loss modelling, efficiency of individual power components are calculated and plotted in Figure 3. Figure also shows the calculated efficiency curve for the converter.

## 5. EXPERIMENTAL RESULTS

The hardware prototype of a 1.7 kW Isolated bidirectional dc-dc converter is shown in Figure 4. The proposed converter is realized on a PCB having size of 14.3cm in length and 7.7cm in width.

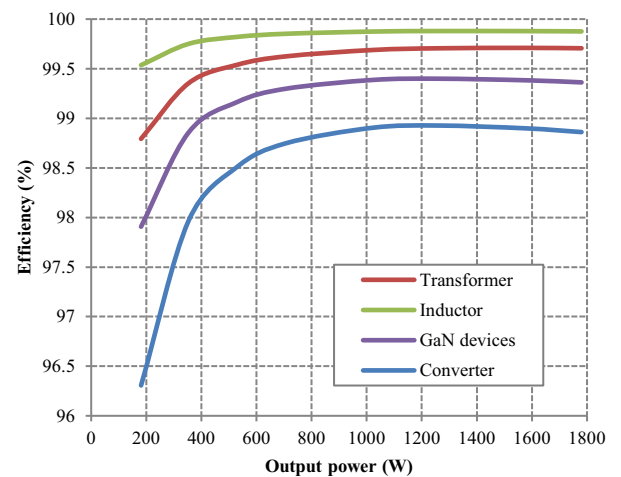


Figure 3. Calculated efficiency curve of the converter along with the efficiency curve of power components

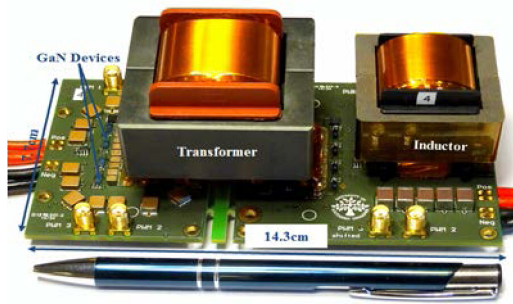


Figure 4. Hardware prototype of the bidirectional isolated dc-dc converter

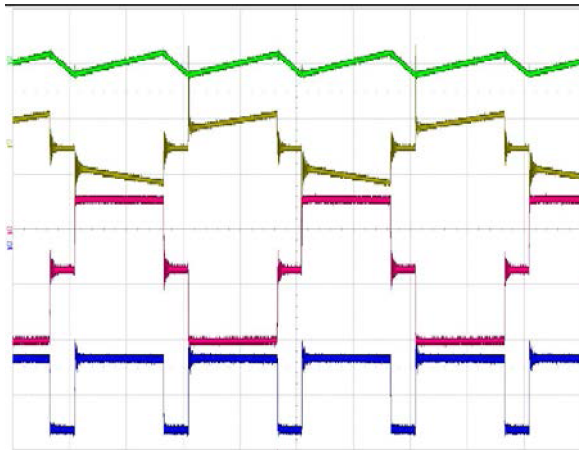


Figure 5. Measured waveforms of the bidirectional dc-dc converter in buck mode of operation (Green: Inductor current 20A/div, Yellow: Transformer primary current 20A/div, Red: Transformer primary voltage 100V/div, Blue: Rectifier voltage 50V/div, Time scale: 5µs/div)

When the efficiency becomes higher, for e.g. above 95%, extensive care has to be taken to measure the efficiency precisely and accurately. Current measurement is performed using a highly stable and precise sense

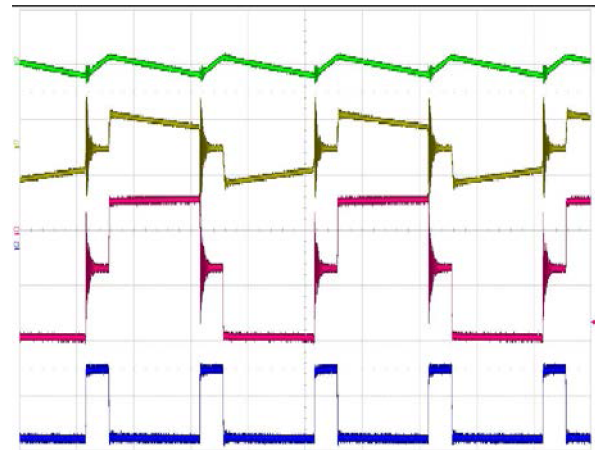


Figure 6. Measured waveforms of the bidirectional dc-dc converter in boost mode of operation (Green: Inductor current 20A/div, Yellow: Transformer secondary current 20A/div, Red: Transformer secondary voltage 100V/div, Blue: Rectifier voltage 50V/div, Time scale: 5µs/div)

resistors and voltage is measured using Keysight’s high precision digital multi-meters.

The bidirectional operation of the converter is verified by operating the converter in buck mode and then in boost mode. In buck mode of operation, high voltage side is connected with a voltage source of 130V and an electronic load is connected at the low voltage side.

In boost mode of operation, the low voltage side is connected with a voltage source of 52V and the high voltage side is connected with an electronic load. The operational waveforms of the converter in both buck and boost mode are measured and shown in Figure 5 and Figure 6, respectively.

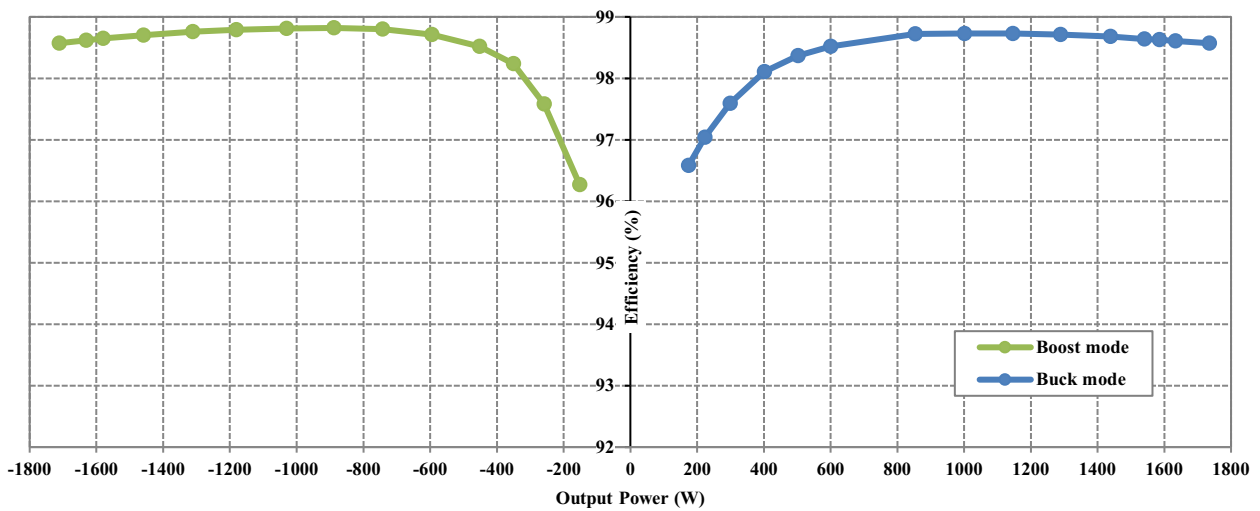


Figure 7. Measured efficiency curve of the bidirectional isolated dc-dc converter

The efficiency of the converter, both in buck mode and boost mode of operation are also measured and plotted in Figure 7. The isolated bidirectional dc-dc converter has achieved a measured maximum efficiency of 98.8% in buck mode as well as in boost mode of operation. The converter also exhibited a measured efficiency of above 98.5% over a wide operating power range, in both directions of power flow.

## 6. CONCLUSION

This paper presents the design and implementation of an isolated bidirectional dc-dc converter. Due to zero reverse recovery losses in GaN FETs, they are used as switching devices to improve the efficiency of the bidirectional dc-dc converter with synchronous rectification.

The design consideration for high efficiency magnetics as well as GaN devices are discussed in this paper. The analytical loss modelling of the individual power components along with calculated efficiency curve for the converter is presented in the paper. The measured efficiency curve of the converter is also shown in the paper. The converter has achieved a measured maximum efficiency of 98.8% in both buck and boost mode of operation. The efficiency of the isolated bidirectional converter is above 98.5% over a wide range of output power.

## 7. ACKNOWLEDGMENT

The project is sponsored by the Danish National Advanced Technology Foundation under Intelligent Efficient Power Electronics (IEPE), strategic research center between the industries and universities in Denmark.

## 8. REFERENCES

1. Kankam, M. D. & Elbuluk, M. E. (2001). A Survey of Power Electronics Applications in Aerospace Technologies. In Proc. 36th Intersociety Energy Conversion Engineering Conference, Savannah, Georgia.
2. Weinberg, A. H. & Schreuders, J. (1986). A High-power High-voltage dc-dc Converter for Space Applications. In Proc. IEEE Transactions on Power Electronics, pp.148-160.
3. Kaminski N. (2009). State of the art and the future of wide band-gap devices. In Proc. 13th European Conference on Power Electronics and Applications, pp. 1-9.
4. Millan J. et al. (2014) A survey of wide bandgap power semiconductor devices. In Proc. IEEE Trans. on Power Electronics, pp. 2155– 2163.
5. Chiu, H. J. & Lin, L. W. (2006). A Bidirectional dc-dc Converter for Fuel Cell Electric Vehicle Driving System. In Proc. IEEE Trans. Power Electron., pp. 950-958.
6. Jiang, T. et al. (2015). A Bidirectional LLC Resonant Converter with Automatic Forward and Backward Mode Transition. In Proc. IEEE Transactions on Power Electronics, pp. 757-770
7. Yu, X. & Yeaman, P. (2014). A New High Efficiency Isolated Bi-directional dc-dc Converter for DC-bus and Battery-bank Interface. In Proc. 29th Applied Power Electronics Conference and Exposition (APEC), pp. 879-883.
8. Ramachandran, R. et al. (2014). Design of a Compact, ultra-high Efficient Isolated dc-dc Converter utilizing GaN Devices. In Proc. 40th Annual Conference of the IEEE Industrial Electronics Society, IECON, pp. 4256-4261.
9. Nymand, M. & Andersen, M. A. E. (2010). High-efficiency Isolated Boost dc-dc Converter for High-power Low-voltage Fuel Cell Applications. In Proc. IEEE Trans. Ind. Electron., pp. 505-514.
10. LM5114 datasheet, Peak current low-side gate driver, (www.ti.com)
11. Nymand, M. et al. (2009). Reducing ac-winding losses in High-current High-power Inductors. In Proc. 35th IEEE IECON Conf., Portugal, pp. 774-778.
12. Steinmetz, C. P. (1984). On the Law of Hysteresis. In Proc. IEEE, pp. 197 -221.
13. Ramachandran R. & Nymand M. (2015). Analysis of Capacitive Losses in GaN Devices for an Isolated Full Bridge DC-DC Converter In Proc. International Conf. on Power Electronics and Drive Systems, pp. 467-472.